

Interplay of electronic structure and atomic ordering on surfaces: Momentum-resolved measurements of Cs atoms adsorbed on a Ag(111) substrate

Hendrik Bentmann,^{1,2} Arne Buchter,^{1,*} and Friedrich Reinert^{1,2}

¹*Experimentelle Physik VII and Röntgen Research Center for Complex Materials (RCCM), Universität Würzburg Am Hubland, D-97074 Würzburg, Germany*

²*Karlsruhe Institute of Technology KIT, Gemeinschaftslabor für Nanoanalytik, D-76021 Karlsruhe, Germany*

(Received 9 February 2012; revised manuscript received 15 March 2012; published 26 March 2012)

Surface-state mediated interactions between adsorbates on surfaces can be exploited for the fabrication of self-organized nanostructures such as two-dimensional superlattices of adatoms. Using angle-resolved photoemission, we provide experimental evidence that these interactions can be drastically modified by adsorbate-induced alterations in the surface potential barrier. This, in turn, will cause significant changes in the ordering of the adsorbates. For the studied case example of Cs adatoms on Ag(111), our momentum-resolved measurements reveal the surface-state Fermi wave vector to be increased by as much as $\sim 100\%$ for coverages around 0.03 ML. Our results unravel the origin for the hitherto puzzling and unexpectedly small lattice constant in the adatom superlattice observed for this system.

DOI: [10.1103/PhysRevB.85.121412](https://doi.org/10.1103/PhysRevB.85.121412)

PACS number(s): 73.20.At, 68.43.Fg

The self-assembly of atoms, molecules, or clusters on surfaces is a prerequisite for the bottom-up approach to the fabrication of ordered low-dimensional nanostructures. The interest in such processes is widespread: it reaches from improvements in the growth quality of organic molecular thin films for enhanced device performances¹ to the design of model systems with tunable interaction parameters for the investigation of new electronic or magnetic effects.²⁻⁶ The structural ordering of adsorbates is often determined by a complex interplay of competing mutual interactions, which may act directly between the adsorbates or via the supporting substrate.⁷⁻⁹ The controlled preparation of tailored structures thus requires understanding of the involved microscopic mechanisms.^{10,11} Here, we address specific types of interactions acting between adatoms and molecules on surfaces which are mediated by surface-state electrons.¹² The mediated interactions can be electronic, as found for the surfaces of different metal substrates,^{13,14} but also magnetic, as predicted for impurities with magnetic moments on topological insulator and metal surfaces.^{15,16} As we will show, such interactions are not necessarily a genuine property of the substrate surface, but instead can exhibit substantial dependence on the adsorbate type and coverage.

Surface-state mediated interactions result from the scattering of surface electrons at adatoms, which gives rise to spatial oscillations in the local density of states (LDOS) of the surface state around the scattering impurity.^{17,18} This effect induces an oscillatory interaction potential between two given adatoms, whereas the oscillation period is directly linked to the surface-state Fermi wave vector of the particular substrate. Scanning tunneling microscopy (STM) experiments very successfully confirmed these predictions for several adatom species on different noble-metal substrates hosting Shockley-type surface states.^{13,14} A particularly interesting consequence of the surface-state mediated interaction potential is the possibility to create well-ordered adatom superlattices, potentially useful for studying magnetic coupling in low dimensions (see, for example, Ref. 19 for a recent review). Experiments for Ce superlattices on Ag(111) and Cu(111)

corroborated a clear correspondence between the equilibrium interatomic distances in these structures and the respective surface-state Fermi wave vector.^{20,21} On the other hand, Cs superlattices on the same substrates were revealed to show markedly reduced interatomic distances compared to the respective Ce counterpart,^{22,23} indicative of additional, unexplored effects taking place in this case.

In this Rapid Communication, we demonstrate that the surface-state mediated potential on a particular substrate can be altered significantly by the presence of adatoms and, moreover, can be tuned as a function of the adatom coverage. This effect arises from adsorbate-induced changes in the surface potential barrier, which give rise to drastic modifications in the Fermi wave vector and the binding energy of the surface-state electrons. To access these important quantities experimentally, we employed angle-resolved photoelectron spectroscopy (ARPES), which is a surface-sensitive technique and allows for the direct measurement of the k -resolved surface electronic structure. As a case study, we present experiments for Cs atoms adsorbed on a Ag(111) substrate for coverages up to 0.06 monolayer (ML). For coverages above 0.03 ML, we find the Fermi wave vector of the Ag(111) surface state to be increased by $\sim 100\%$ compared to the value for the clean surface. This remarkable observation gives a conclusive and quantitative explanation for the as yet surprisingly small lattice constant for the Cs superlattice on Ag(111).²³ Our results thus disclose an important aspect of surface-state mediated ordering which can be essential for a proper understanding of the resulting adsorbate geometry. In turn, the mechanism provides possibilities to tune electronic or magnetic interactions and corresponding ordering phenomena in low-dimensional nanostructures.

We performed high-resolution ARPES experiments employing a Scienta R4000 electron analyzer and a microwave-driven He-discharge lamp (MB-Scientific). The angular and energy resolution of the setup were set to 0.3° and 8 meV. For all presented measurements, we used an excitation energy of $h\nu = 21.22$ eV (He I). The experiments were carried out under ultrahigh vacuum conditions with a base pressure below 2×10^{-10} mbar and at a sample temperature of ~ 20 K.

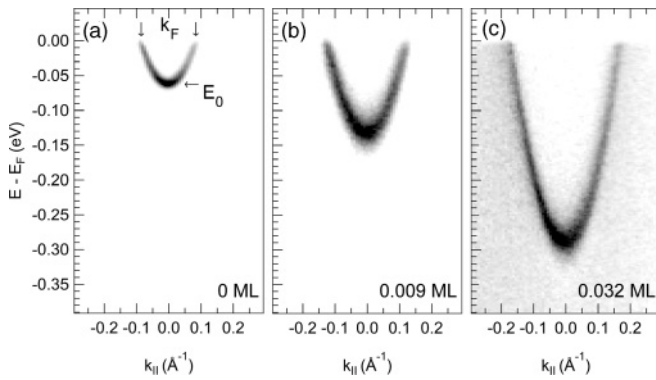


FIG. 1. Angle-resolved photoemission for the clean (a) and Cs-covered (b), (c) Ag(111) surface around the Γ point ($k_{\parallel} = 0 \text{ \AA}^{-1}$). Fermi momentum k_F and binding energy E_0 of the parabolic surface-state dispersion are largely influenced by the Cs-induced modification of the surface potential barrier.

The Ag(111) single crystal was prepared by standard sputter-annealing cycles. The surface quality was characterized by ARPES measurements of the surface-state linewidth (see Ref. 24) and with low-energy electron diffraction (LEED). Commercial alkali sources (SAES getters S.p.A.) were employed for Cs deposition. The deposition rate was gauged using the Cs-induced ($\sqrt{3} \times \sqrt{3}$) reconstruction occurring at a coverage of 1/3 ML (see Ref. 25) and is estimated to be accurate within $\pm 20\%$.

The electronic structure of the pristine Ag(111) surface features a surface state in the bulk-projected energy gap around the Γ point of the surface Brillouin zone [Fig. 1(a)]. Its parabolic dispersion is specified by the Fermi wave vector k_F and the maximum binding energy E_0 for which we determine values of 0.085 \AA^{-1} and 62 meV, in agreement with previous experiments.²⁴ As inferred from Figs. 1(b) and 1(c), successive deposition of impurity concentrations of Cs adatoms gives rise to a steady increase in the binding energy E_0 of the surface state. This pronounced dispersion modification results from the sensitivity of surface states to changes in the surface potential. When bound to a surface, alkali atoms tend to form comparably large dipole moments, which result in significant reductions of the substrate work function.²⁶ Based on STM measurements on Cs/Ag(111), a work function change $\Delta\phi \approx 1 \text{ eV}$ has been determined for $\theta = 0.03\text{--}0.04 \text{ ML}$.²³ By employing a simple phase analysis model to take into account the changed surface barrier (see Refs. 27–29) and using this value for $\Delta\phi$, we estimate a surface-state binding energy increase of $\sim 200 \text{ meV}$, which is in good agreement with our experimental data in Fig. 1(c). The large change in E_0 is therefore mainly attributed to modifications in the surface potential barrier due to the Cs adsorption, whereas also direct doping most likely has an additional but smaller effect. We stress that the observation of a single well-defined surface-state band for the Cs-covered samples indicates a homogeneous distribution of the Cs adatoms without island formation.³⁰ This is indeed expected because of the dipole-dipole repulsion between the adsorbed atoms.

A crucial consequence of the observed binding-energy increase is the associated changes of the surface-state Fermi wave vector k_F . In Fig. 2, we consider momentum distribution

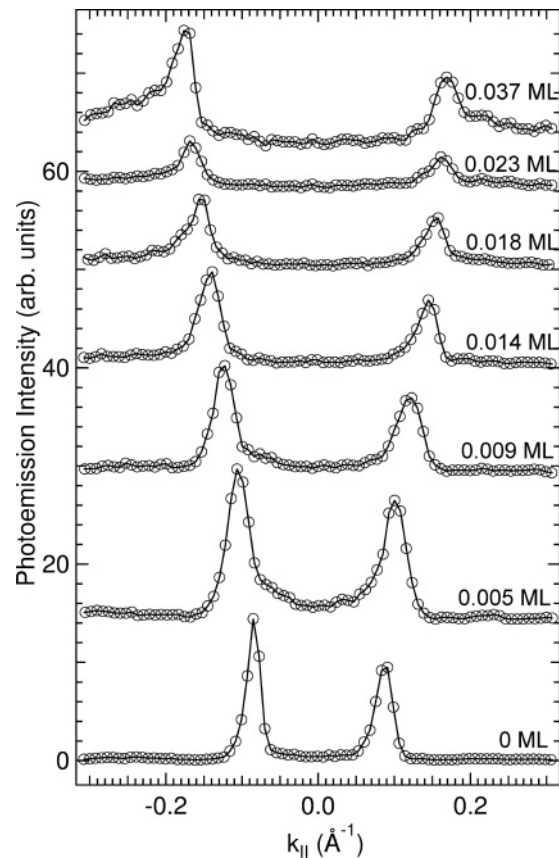


FIG. 2. Momentum distribution curves at the Fermi energy E_F for the Ag(111) surface state for increasing Cs coverage. The data evidence a coverage-dependent enhancement of the surface-state Fermi wave vector k_F . The asymmetry in the peak intensities results from photoemission matrix element effects.

curves (MDCs) taken at the Fermi energy E_F for rising amounts of Cs coverage. The two peaks in each spectrum correspond to the Fermi wave vector in the $\pm k_{\parallel}$ directions. The data indicate shifts of the two peaks to larger k_{\parallel} values and thus a gradual enhancement of the Fermi wave vector with increasing Cs concentration on the surface. The results of the full data set are summarized in Fig. 3, where we plot the measured surface-state parameters k_F and E_0 as a function of the Cs coverage in Figs. 3(a) and 3(b). Both parameters show a similar coverage dependence: Up to $\sim 0.02 \text{ ML}$, we find a linear increase which is maintained but reduced for

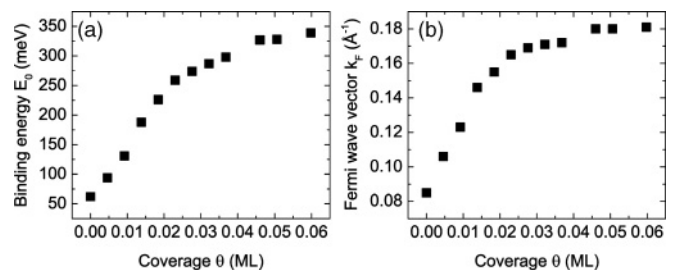


FIG. 3. Full data set on the coverage dependence of the surface-state parameters E_0 in (a) and k_F in (b) corresponding to the representative data plots in Figs. 1 and 2. The symbol sizes in (a) and (b) exceed the experimental error along the ordinate axis.

higher coverages. The most important finding for this work is that already at a Cs coverage of ~ 0.03 ML, the surface-state Fermi wave vector is enhanced by a factor >2 and the binding energy is enhanced by a factor >4 when compared to values of the clean Ag(111) surface. It is important to note that the observed surface-state modifications eventually result from chemisorptive, partially ionic Cs-Ag bonds with binding energies on the eV scale.²⁶ Therefore, we do not expect a significant temperature dependence of the above findings in the low-temperature regime below ~ 100 K.

In the following, we will discuss the implications of the experimentally determined coverage dependence of the surface-state parameters k_F and E_0 for surface-state mediated interactions between impurities and a resulting superlattice formation. To this end, we will compare our present results to previous STM experiments, which observed the formation of a Cs adatom superlattice on Ag(111) at a coverage of 0.03–0.04 ML and a temperature of 7 K.²³ The superlattice constant deduced in these experiments was $d_{Cs} = (15 \pm 2)$ Å and hence considerably reduced as compared to the Ce superlattice on Ag(111) where $d_{Ce} = (32 \pm 2)$ Å was found.²⁰

The oscillating interaction energy between two adatoms due to surface-state scattering is given by

$$E_i^s = -AE_0 \left(\frac{2 \sin(\delta_0)}{\pi} \right)^2 \frac{\sin(2k_F|r_1 - r_2| + 2\delta_0)}{(k_F|r_1 - r_2|)^2}, \quad (1)$$

with the scattering amplitude A and the scattering phase δ_0 .¹⁸ It is important to note that the form of E_i^s depends crucially on k_F and E_0 and hence is expected to change significantly if these parameters are modified. In addition to E_i^s , the repulsive dipole-dipole interaction energy

$$E_i^d = \frac{1}{4\pi\epsilon_0} \frac{p^2}{|r_1 - r_2|^3} \quad (2)$$

between two adatoms with the dipole moment p must be taken into account to obtain the total interaction energy $E_i = E_i^s + E_i^d$. In Ref. 23, the parameters $A \approx 0.3$, $\delta_0 \approx 0.5\pi$, and $p \approx (0.9 \pm 0.3) e \text{ Å}$ were estimated for Cs/Ag(111). Using these values, we are able to compute the interaction energy E_i between two Cs atoms on the Ag(111) surface for the measured parameter pairs of k_F and E_0 (Fig. 3).

In Fig. 4, we plot E_i for the surface-state parameters of the clean surface (dashed line) and for the ones obtained by our measurements for $\theta = 0.032$ ML (full line). The most important parameter in these curves is the location of the first energy minimum d_m as for this interatomic distance, the formation of an energetically stabilized superlattice is possible. Clearly, for the parameters of the clean surface, d_m largely deviates from the lattice constant of 15 Å found in Ref. 23 (see shaded area in Fig. 4). However, using the redetermined values from our ARPES study, the agreement is striking. We find $d_m \approx 14$ Å, which fully coincides with the previously observed superlattice constant within experimental uncertainty. The large change in d_m results from the modification of the Fermi wave vector after Cs deposition. Note that the distance d_m does not only depend on k_F , but also on the scattering phase δ_0 , the choice of which constitutes the largest uncertainty in the present determination of d_m . Previous investigations found scattering phases of 0.33π and 0.37π for Co and Ce atoms on

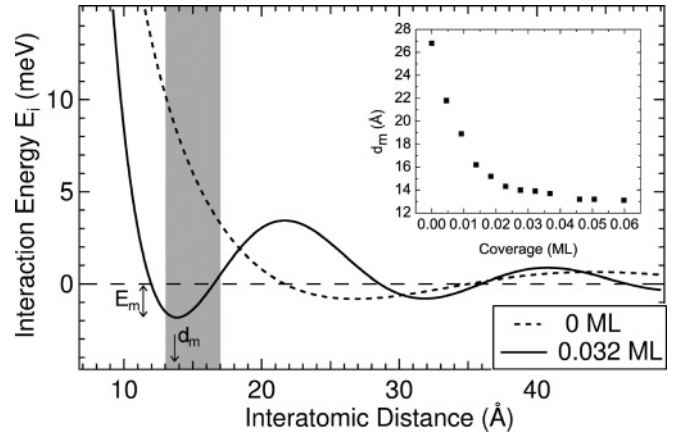


FIG. 4. Calculated adatom interaction energy E_i using surface-state parameters of the clean surface ($k_F = 0.085 \text{ Å}^{-1}$, $E_0 = 62 \text{ meV}$; dashed line) and of the Cs-covered surface for $\theta = 0.032$ ML ($k_F = 0.171 \text{ Å}^{-1}$, $E_0 = 287 \text{ meV}$; full line). The shaded area represents the Cs superlattice constant, including the experimental error found by STM experiments (Ref. 23). The inset shows the calculated position d_m of first energy minimum E_m (see text for details) as a function of the Cs coverage θ . All calculations are done for $\delta_0 = 0.5\pi$.

Ag(111).^{14,20} Assuming according reductions in δ_0 , we obtain $d_m \approx 16$ – 17 Å. The agreement with the STM experiments is thus maintained for a plausible range of scattering phases, whereas optimal correspondence ($d_m \approx 15$ Å) is found for $\delta_0 = 0.43\pi$.

Importantly, in addition to the modified Fermi wave vector, also the strong increase of the binding energy E_0 plays an essential role for our considerations. E_0 defines the energy scale in Eq. (1) and therefore determines the actual energy gain E_m for a given scattering phase and amplitude (see Fig. 4). The importance of a sufficiently large ratio between E_m and the adatom diffusion barrier height E_D for the realization of a superlattice has recently been emphasized.³¹ For the system Cs/Ag(111), $E_D \approx 17 \text{ meV}$ was determined in Ref. 23. Using this number, we obtain values for E_m/E_D in the range of $\sim 7\%$ – 12% for scattering phases δ_0 between 0.37π and 0.5π . Note here that E_m , unlike d_m , additionally shows a strong dependence on the scattering amplitude A and the dipole moment p , rendering our calculated values as a rough estimation. Nevertheless, the numbers we obtain agree with those observed for other adsorbate-substrate combinations which were shown to stabilize adatom superlattices where one typically finds $E_m/E_D > 6\%$.³¹ The strong enhancement of E_0 with Cs adsorption can therefore be identified as an effect of critical importance for the energetical stabilization of the superlattice.

Taken collectively, our experimental results provide a comprehensive explanation for the observation of a Cs superlattice on Ag(111) with a lattice constant of 15 Å and a coverage of 0.03–0.04 ML. We deduce that the structural ordering in this system is not solely determined by the substrate but additionally by the adsorbate itself, which decisively influences the surface-state mediated interaction. It is instructive to examine the coverage dependence of the equilibrium distance d_m obtained from the data in Fig. 3 (see inset in Fig. 4). It turns out that the energy minimum distance of the adatom interaction

energy varies over a considerable range between 13 and 27 Å. This demonstrates a possibility to tune surface-state mediated interactions between surface adatoms, in addition to a change of the substrate.¹⁴

As several previous studies on different noble metals reported surface-state modifications for a variety of different adsorbate species, the findings presented here are likely to have consequences for a broad range of material systems (see, e.g., Ref. 11). Generally, electropositive species, such as alkali atoms studied here, tend to increase the surface-state binding energy E_0 and Fermi wave vector k_F .³² However, also the opposite effect, that is, a reduction of E_0 and k_F , has been observed, for example, for the adsorption of CO molecules,³³ rare gases,³⁴ or dielectric NaCl overlayers³⁵ on noble-metal surfaces. In this case, an enhancement of the equilibrium distance d_m should be expected. For possible implications of our work, we point out a number of recent studies on atomic or molecular superstructures on metal surfaces for which a significant change in the surface-state dispersion due to dipole formations may be expected.^{19,36,37} Interestingly, another investigation reports variations in the distance distributions for different organic and inorganic molecules on Cu(111) depending on their dipole moments.³⁸ One can anticipate that

the mechanism established in our work plays an important role for these observations. Furthermore, adsorption experiments on topological insulators find modifications in the surface electronic structure upon adatom coverage, suggesting that similar effects as discussed here will also be relevant for the surface-state mediated Ruderman-Kittel-Kasuya-Yosida (RKKY) interactions and resulting surface magnetism predicted for these systems.^{15,39,40}

We have established a mechanism in the adsorbate-substrate interplay in low-dimensional surface nanostructures which, as we have shown, can radically change the involved interactions between adsorbates. In particular, surface-state mediated interactions are found to be modified upon adsorbate deposition. This is due to the sensitivity of surface states to changes in the vacuum-surface potential barrier. The findings offer a way to manipulate the self-assembly of atoms or molecules on surfaces.

We acknowledge helpful discussions with M. Bode, F. Forster, and M. Mulazzi. This work was supported by the Bundesministerium für Bildung und Forschung (Grants No. 05K10WW1/2 and No. 05KS1WMB/1) and the Deutsche Forschungsgemeinschaft within the Forschergruppe 1162.

*Present address: Department of Physics, University of Basel, Klingelbergstr. 82, CH-4056 Basel, Switzerland.

¹Y. D. Park, J. A. Lim, H. S. Lee, and K. Cho, *Mater. Today* **10**, 46 (2007).

²C. Blumenstein, J. Schäfer, S. Mietke, S. Meyer, A. Dollinger, M. Lochner, X. Y. Cui, L. Patthey, R. Matzdorf, and R. Claessen, *Nat. Phys.* **7**, 776 (2011).

³M. Bode, M. Heide, K. von Bergmann, P. Ferriani, S. Heinze, G. Bihlmayer, A. Kubetzka, O. Pietzsch, S. Blügel, and R. Wiesendanger, *Nature (London)* **447**, 190 (2007).

⁴P. Gambardella, S. Stepanow, A. Dmitriev, J. Honolka, F. M. F. de Groot, M. Lingenfelder, S. S. Gupta, D. D. Sarma, P. Bencok, S. Stanescu *et al.*, *Nat. Mater.* **8**, 189 (2009).

⁵K. Sakamoto, T. Oda, A. Kimura, K. Miyamoto, M. Tsujikawa, A. Imai, N. Ueno, H. Namatame, M. Taniguchi, P. E. J. Eriksson *et al.*, *Phys. Rev. Lett.* **102**, 096805 (2009).

⁶Z. M. Abd El-Fattah, M. Matena, M. Corso, F. J. Garcia de Abajo, F. Schiller, and J. E. Ortega, *Phys. Rev. Lett.* **107**, 066803 (2011).

⁷Y. Wang, X. Ge, C. Manzano, J. Kröger, R. Berndt, W. A. Hofer, H. Tang, and J. Cerda, *J. Am. Chem. Soc.* **131**, 10400 (2009).

⁸C. Stadler, S. Hansen, I. Kröger, C. Kumpf, and E. Umbach, *Nat. Phys.* **5**, 153 (2009).

⁹R. Otero, J. M. Gallego, A. L. V. de Parga, N. Martin, and R. Miranda, *Adv. Mater.* **23**, 5148 (2011).

¹⁰J. V. Barth, G. Costantini, and K. Kern, *Nature (London)* **437**, 671 (2005).

¹¹F. Forster, A. Bendounan, J. Ziroff, and F. Reinert, *Surf. Sci.* **600**, 3870 (2006).

¹²P. Han and P. S. Weiss, *Surf. Sci. Rep.* **67**, 19 (2012).

¹³J. Repp, F. Moresco, G. Meyer, K. H. Rieder, P. Hyldgaard, and M. Persson, *Phys. Rev. Lett.* **85**, 2981 (2000).

¹⁴N. Knorr, H. Brune, M. Epple, A. Hirstein, M. A. Schneider, and K. Kern, *Phys. Rev. B* **65**, 115420 (2002).

¹⁵Q. Liu, C.-X. Liu, C. Xu, X.-L. Qi, and S.-C. Zhang, *Phys. Rev. Lett.* **102**, 156603 (2009).

¹⁶V. S. Stepanyuk, L. Niebergall, R. C. Longo, W. Hergert, and P. Bruno, *Phys. Rev. B* **70**, 075414 (2004).

¹⁷M. F. Crommie, C. P. Lutz, and D. M. Eigler, *Nature (London)* **363**, 524 (1993).

¹⁸P. Hyldgaard and M. Persson, *J. Phys.: Condens. Matter* **12**, L13 (2000).

¹⁹M. Ternes, M. Pivetta, F. Patthey, and W.D. Schneider, *Prog. Surf. Sci.* **85**, 1 (2010).

²⁰F. Silly, M. Pivetta, M. Ternes, F. Patthey, J. P. Pelz, and W. D. Schneider, *Phys. Rev. Lett.* **92**, 016101 (2004).

²¹N. N. Negulyaev, V. S. Stepanyuk, L. Niebergall, P. Bruno, M. Pivetta, M. Ternes, F. Patthey, and W.-D. Schneider, *Phys. Rev. Lett.* **102**, 246102 (2009).

²²T. von Hofe, J. Kröger, and R. Berndt, *Phys. Rev. B* **73**, 245434 (2006).

²³M. Ziegler, J. Kröger, R. Berndt, A. Filinov, and M. Bonitz, *Phys. Rev. B* **78**, 245427 (2008).

²⁴F. Reinert, G. Nicolay, S. Schmidt, D. Ehm, and S. Hüfner, *Phys. Rev. B* **63**, 115415 (2001).

²⁵G. S. Leatherman and R. D. Diehl, *Phys. Rev. B* **53**, 4939 (1996).

²⁶H. Bonzel, *Surf. Sci. Rep.* **8**, 43 (1988).

²⁷P. Echenique and J. Pendry, *Prog. Surf. Sci.* **32**, 111 (1989).

²⁸A. Nuber, M. Higashiguchi, F. Forster, P. Blaha, K. Shimada, and F. Reinert, *Phys. Rev. B* **78**, 195412 (2008).

²⁹N. V. Smith, *Phys. Rev. B* **32**, 3549 (1985).

³⁰H. Cercellier, C. Didiot, Y. Fagot-Revurat, B. Kierren, L. Moreau, D. Malterre, and F. Reinert, *Phys. Rev. B* **73**, 195413 (2006).

³¹X. P. Zhang, B. F. Miao, L. Sun, C. L. Gao, A. Hu, H. F. Ding, and J. Kirschner, *Phys. Rev. B* **81**, 125438 (2010).

³²S. Å. Lindgren and L. Walldén, *Solid State Commun.* **28**, 283 (1978).

- ³³S. Å. Lindgren, J. Paul, and L. Walldén, *Surf. Sci.* **117**, 426 (1982).
- ³⁴H. Hövel, B. Grimm, and B. Reihl, *Surf. Sci.* **477**, 43 (2001).
- ³⁵J. Repp, G. Meyer, and K.-H. Rieder, *Phys. Rev. Lett.* **92**, 036803 (2004).
- ³⁶T. Yokoyama, T. Takahasi, K. Shinozaki, and M. Okamoto, *Phys. Rev. Lett.* **98**, 206102 (2007).
- ³⁷I. Fernandez-Torrente, S. Monturet, K. J. Franke, J. Fraxedas, N. Lorente, and J. I. Pascual, *Phys. Rev. Lett.* **99**, 176103 (2007).
- ³⁸M. Mehlhorn, V. Simic-Milosevic, S. Jaksch, P. Scheier, and K. Morgenstern, *Surf. Sci.* **604**, 1698 (2010).
- ³⁹L. A. Wray, S. Xu, Y. Xia, D. Hsieh, A. V. Fedorov, Y. S. Hor, R. J. Cava, A. Bansil, H. Lin, and M. Z. Hasan, *Nat. Phys.* **7**, 32 (2011).
- ⁴⁰J.-J. Zhu, D.-X. Yao, S.-C. Zhang, and K. Chang, *Phys. Rev. Lett.* **106**, 097201 (2011).